JOURNAL OF CATALYSIS 87, 98–107 (1984)

Nonoxidative Dehydrogenation of Ethylbenzene over TiO_2–ZrO_2 Catalysts

II. The Effect of Pretreatment on Surface Properties and Catalytic Activities

JUNG-CHUNG WU,* CHUNG-SUN CHUNG,*,[1] CHING-LAN AY,† AND IKAI WANG†

*Departments of *Chemistry and †Chemical Engineering, National Tsing Hua University, Hsinchu, Taiwan, Republic of China*

Received July 15, 1983; revised November 17, 1983

Catalytic activities for the nonoxidative dehydrogenation of ethylbenzene were determined for TiO_2–ZrO_2 catalysts which had been calcined at temperatures between 550 and 1000°C. The acidic and basic properties and surface areas of these catalysts were also measured. The change of crystal structure with calcination temperatures was studied by XRD analysis. The maximum of catalytic activity was obtained by calcination at about 650°C with an equal-molar ratio of TiO_2 and ZrO_2. This high activity may be due to the formation of $ZrTiO_4$ crystal. The activity of the catalyst was poisoned not only by K_2O but also by H_3BO_3. Based on the effects of pretreatment with H_2, O_2, and steam, structures are proposed for the catalytically active sites. It is concluded that the formation of $ZrTiO_4$ crystal as well as the amounts of acid and base sites are the major factors affecting the catalytic activity.

INTRODUCTION

By studying the isomerization of 1-methylcyclohexene oxide, TiO_2–ZrO_2 has been shown to be an effective acid–base bifunctional catalyst (*1, 2*). In a previous paper (*3*), we proposed a two-center mechanism for ethylbenzene dehydrogenation over TiO_2–ZrO_2 catalysts based on the following evidence: (1) the activity correlated well with the amounts of acid and base; (2) the activity was poisoned not only by K_2O but also by H_3BO_3. Similar acid–base bifunctional mechanisms have also been proposed for the oxidative dehydrogenation of ethylbenzene by Murakami (*4, 5*), and for the conversion of alcohols to ethers over reduced nickel oxide or Pt–Cab–O–Sil catalyst by Pines (*6–9*).

Polycrystalline zirconium titanate has been investigated as a high-temperature dielectric material by other researchers who found that ceramic $ZrTiO_4$ could be obtained by direct reaction of TiO_2 and ZrO_2 at high temperatures (1200–1700°C) (*10–14*). Synthesis of zirconium titanate from coprecipitated titanium and zirconium compounds by thermal decomposition or spray-drying has also been reported (*15–17*). However, the effect of pretreatment on surface properties and catalytic activities of these catalysts have not been reported.

Recently, we have studied the crystal structures of TiO_2–ZrO_2 (1/1) calcined at various temperatures, the acid–base properties of these catalysts, their catalytic activity for dehydrogenation of ethylbenzene, the effects of pretreatment with H_2, O_2, and steam on these catalysts, and the structures of the active sites on these catalysts. The results are reported herein.

EXPERIMENTAL

Preparation of Catalysts

An anhydrous alcohol solution which contained equal moles of titanium tetra-

[1] To whom correspondence should be addressed at the National Tsing Hua University.

0021-9517/84 $3.00

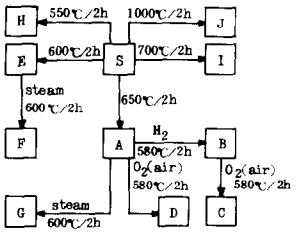

SCHEME 1

chloride and zirconium tetrachloride was added to 28% aqueous ammonia. The precipitate was aged over water bath for 2 hr, washed with deionized water until no chloride ions were detected in the filtrate, and then dried at 110°C. The dried precipitate was calcined at various temperatures between 550 and 1000°C for 2 hr. A solid obtained by coprecipitation of equal moles of $TiCl_4$ and $ZrCl_4$ was dried at 110°C and denoted as S. The pretreatments of the solid S are shown in Scheme 1.

Ethylbenzene Adsorption Measurement

The amount of adsorption of ethylbenzene over the catalysts with various compositions was measured by a Perkin–Elmer TGS-2 apparatus. The vapor of ethylbenzene, which was carried by nitrogen gas, passed continuously through the catalysts sample at 150°C. The weight gain of the sample was considered as the amount of adsorption.

Acidity and Basicity Measurement

The acidity and basicity of the catalysts were measured by n-butylamine and acetic acid adsorption, respectively. The catalyst was first put in a desiccator with saturated *n*-butylamine or acetic acid vapor at room temperature for 48 hr. Then, the weight loss of the adsorbed sample was measured by a TG apparatus.

Surface Area and X-Ray Analysis

The specific surface area of catalysts was determined by applying the BET method. Crystalline of the catalysts was characterized by X-ray powder diffraction pattern over the range of $2\theta = 4$–$60°$ with nickel-filtered Cu$K\alpha$ radiation.

Reaction Equipment and Experimental Procedure

Catalytic reaction was carried out in a continuous flow fixed-bed microreactor as described in a previous paper (*3*). The catalyst bed was first heated up to 580°C with a nitrogen stream at a flow rate of 50 ml/min to remove contamination. Then, the reaction was studied under the following conditions: temperature, 580°C; total pressure, 760 mm Hg (absolute); ethylbenzene partial pressure, 2 mm Hg; H_2O/EB mole ratio, 10; NPT space velocity, 12,000 hr^{-1}. The pore size distributions were obtained by using a Quantachrome Autoscan Porosimeter.

The nonoxidative dehydrogenation of ethylbenzene (EB) over TiO_2–ZrO_2 catalysts gives styrene (ST) as the major product and small amount of benzene and toluene as by-products. In this study, the catalyst performance is shown in the equations:

$$\text{Ethylbenzene conversion, } C(\%) = \frac{\text{EB}_{\text{inlet}} - \text{EB}_{\text{outlet}}}{\text{EB}_{\text{inlet}}} \times 100\%$$

$$\text{Product selectivity, } S_i \text{ (\%, mole)} = \frac{\text{Product } (i)}{\text{EB}_{\text{inlet}} - \text{EB}_{\text{outlet}}} \times 100\%$$

$$\text{Product yield, } Y_i \text{ (\%, mole)} = \frac{\text{Product } (i)}{\text{EB}_{\text{inlet}}} \times 100 = C \times S_i$$

RESULTS AND DISCUSSION

Effect of Calcination Temperature

In a previous paper (*3*) we have proposed an acid–base bifunctional mechanism for nonoxidative dehydrogenation of ethylbenzene over TiO_2–ZrO_2 catalysts calcined at 550°C. The results indicated that the activity for this reaction increased with increasing numbers of acidic and basic sites. From

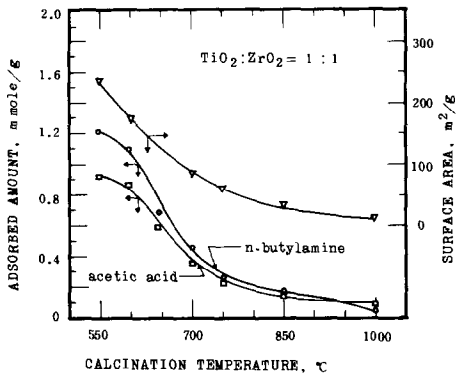

FIG. 1. Surface area and amounts of *n*-butylamine and acetic acid adsorbed over TiO_2–ZrO_2 at various calcination temperatures.

the XRD spectra of TiO_2–ZrO_2 calcined at 550°C with various compositions, we found that TiO_2–ZrO_2 became amorphous if neither the content of TiO_2 or ZrO_2 was less than 25%. The crystallization of these binary oxides was inhibited with each other. The significant changes of surface area, acidity and catalytic activity could be explained by this mutual interaction (*3*).

In the present work, the acidities, basicities, and surface areas of TiO_2–ZrO_2 (1/1) samples calcined at temperatures between 550 and 1000°C were measured by the methods described in above section. Acidity, basicity, and surface area decreased

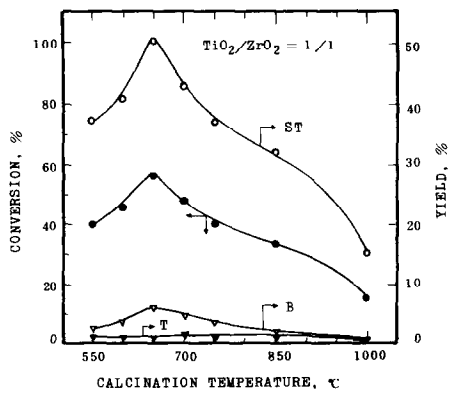

FIG. 2. Total conversion and the yield of the products over TiO_2–ZrO_2 at various calcination temperatures.

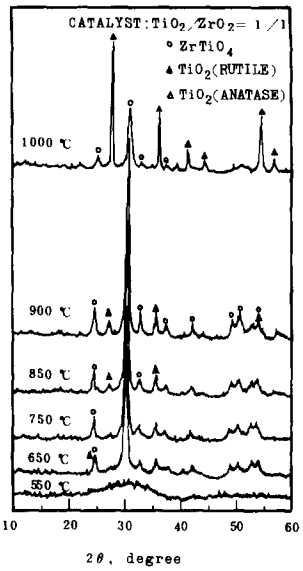

FIG. 3. X-Ray diffraction pattern of TiO_2–ZrO_2 (1/1) at various calcination temperatures.

with increasing calcination temperature, as shown in Fig. 1. Therefore, according to the previously proposed acid–base bifunctional mechanism, the activity for dehydrogenation of ethylbenzene should also decrease with increasing calcination temperature. However, this was not the case. We found that the maximum value of activity was obtained when TiO_2–ZrO_2 (1/1) was calcined at 650°C instead of 550°C, as shown in Fig. 2. Besides the amounts of acid and base there must be another significant factor affecting the catalytic activity.

In order to identify this factor, we studied the crystal structures and pore structures of these catalysts by X-ray powder diffraction and mercury infusion, respectively. Figure 3 shows the XRD patterns of TiO_2–ZrO_2 (1/1) at various calcination temperatures. The crystallines of TiO_2 (rutile), TiO_2 (anatase), and $ZrTiO_4$ were identified by the peaks occurred at 2θ = 27.4(vs), 35.9(s), 41.2(m), 54.3(s); 25.2(vs), 37.8(m), 48.0(m), 53.9(m); and 24.7(m), 30.6(vs), 32.9(m), 42.2(w), respectively (*18*). We found that (1) TiO_2–ZrO_2 (1/1) was amorphous when it was calcined at a tempera-

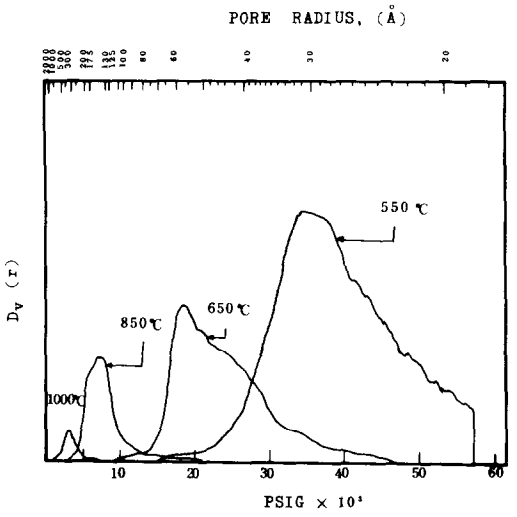

FIG. 4. Pore size distribution over TiO_2–ZrO_2 at various calcination temperatures; mercury penetration method.

ture below 550°C; (2) crystalline $ZrTiO_4$ formed above 650°C and the maximum crystallinity of $ZrTiO_4$ was obtained at 900°C; (3) rutile crystallized gradually when the calcination temperature was above 850°C. In other words, some TiO_2 separated from $ZrTiO_4$ when the calcination temperature was above 850°C. Mizuno has reported that monoclinic ZrO_2 and tetragonal TiO_2 could be formed by the decomposition of $ZrTiO_4$ which was quenched from 2100 to 2400°C (*12*). Nevertheless, as shown in Fig. 3, we did not find the formation of ZrO_2 along with the formation of rutile for TiO_2–ZrO_2 (1/1) calcinated below 1000°C. Perhaps, the content of zirconium oxide in the binary phase increased with increasing calcination temperature. In other words, $Zr_{1+x}TiO_{4+2x}$ formed along with the formation of rutile.

The pore size distributions of the catalysts were measured in the range of 15 and 2000 Å. The results are shown in Fig. 4. It is clear that the average pore size of the catalysts increased with increasing calcination temperature. The mean pore radii are 30, 55, 145, and 400 Å for the catalysts obtained by calcination at 550, 650, 850, and 1000°C, respectively. We also found that the pore volume of the catalysts decreased sharply as the calcination temperature higher than 650°C. These results explained the facts that the surface area and the amounts of acid and base decreased as the calcination temperature increased, as shown in Fig. 1.

From the results of X-ray diffraction study, it is clear that the high activity of the catalyst calcined at 650°C was due to formation of $ZrTiO_4$ crystal. However, if the formation of $ZrTiO_4$ structure were the only factor affecting the activity of ethylbenzene dehydrogenation, the catalysts calcined at 800–900°C would be the most active. Thus, we speculated that both the amounts of acid and base and $ZrTiO_4$ crystallinity are important factors affecting the catalytic activity for nonoxidative dehydrogenation of ethylbenzene over TiO_2–ZrO_2 catalysts.

In our previous work (*3*), we have demonstrated that the acidity and basicity of the catalyst can be poisoned by small amounts of K_2O and B_2O_3, respectively. In this work, the effects of K_2O and B_2O_3 on the catalytic activity were also studied in order to demonstrate the roles of the acid and base centers of the catalysts which were calcined at higher temperatures. Figure 5 shows that the conversion of ethylbenzene and the yield of styrene increase with the addition of a very small amount of H_3BO_3 (0.05–0.1%), and decrease gradually as the

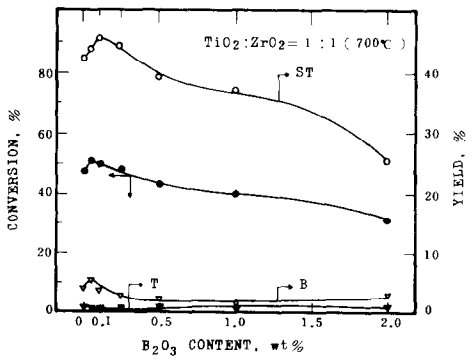

FIG. 5. Effect of doping with B_2O_3 on the total conversion and the yield of the products.

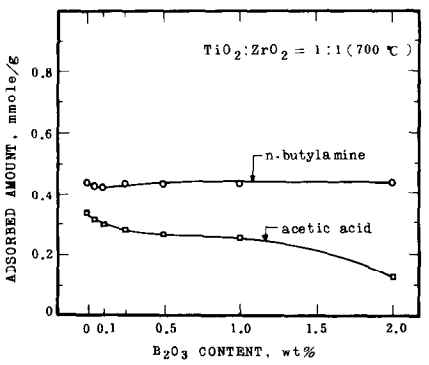

FIG. 6. Effect of doping with B_2O_3 on the adsorbed amounts of *n*-butylamine and acetic acid.

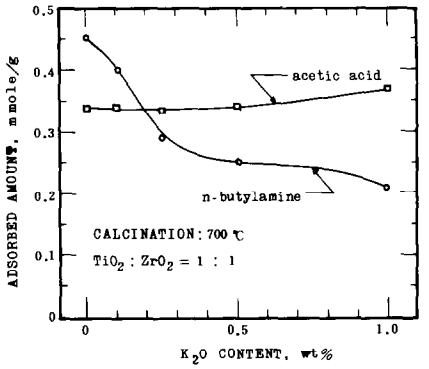

FIG. 8. Effect of doping with K_2O on the adsorbed amounts of *n*-butylamine and acetic acid.

amount of H_3BO_3 is larger than 0.1%. The decreasing of activity is due to the poisoning of basic sites. The change of the adsorbed amount of acetic acid for the addition of H_3BO_3, as shown in Fig. 6, is consistent with the change of catalytic activity. From Fig. 7, we found that the activity decreased drastically through the addition of K_2O in the range of 0.1–1.0%. This decreasing is due to the poisoning of acid sites, as illustrated by the change of the adsorbed amount of *n*-butylamine shown in Fig. 8. Comparing these results with those of our previous work (*3*), we find that the activity is affected by the addition of K_2O and B_2O_3 much more markedly for the catalysts calcined at 700°C than those calcined at 550°C.

The relation between ethylbenzene conversion and the composition of TiO_2–ZrO_2 is shown in Fig. 9, where all the catalysts were calcined at 700°C for 2 hr. The conversions of this reaction over pure ZrO_2 and pure TiO_2 are 6 and 28%, respectively. Both of them are much less than that for the reaction over the binary oxides. From Fig. 9, we found that the maximum activity occurred as the content of TiO_2 was between 50 and 75 mole%. This is not the same as the reaction over catalysts calcined at 550°C, which showed approximately the same activity if the content of either TiO_2 or ZrO_2 was not less than 25% as we reported previously (*3*).

The amounts of acidic and basic sites and ethylbenzene adsorption on TiO_2–ZrO_2 as a function of TiO_2 content were measured and shown in Fig. 10. These results corre-

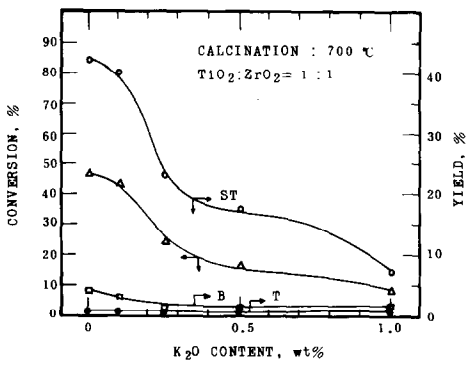

FIG. 7. Effect of doping with K_2O on the total conversion and the yield of the products.

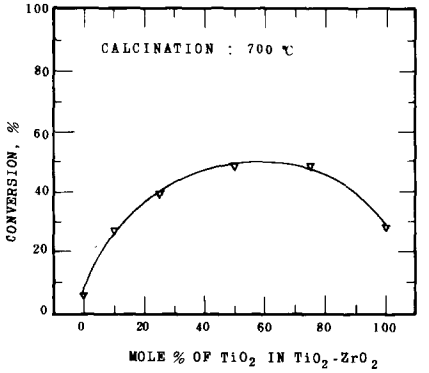

FIG. 9. Activity of ethylbenzene dehydrogenation over TiO_2–ZrO_2 at various compositions.

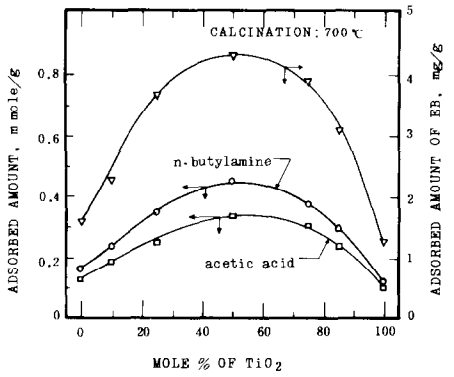

FIG. 10. Amounts of *n*-butylamine, acetic acid, and ethylbenzene adsorbed over TiO_2–ZrO_2 at various compositions.

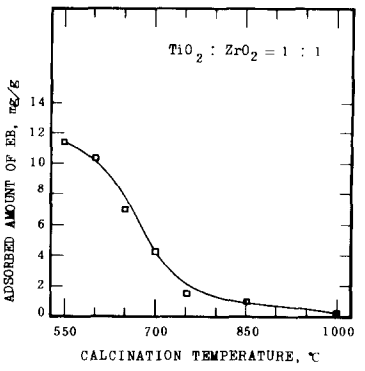

FIG. 12. Amounts of ethylbenzene adsorbed over TiO_2–ZrO_2 at various calcination temperature; adsorption temperature 150°C.

lated well with the catalytic activity. Figure 11 shows the XRD spectra of TiO_2–ZrO_2 with different compositions calcined at 700°C, where crystalline ZrO_2 was identified by the peaks at 2θ = 28.2(vs), 31.5(s), 34.2(m), and 49.3(m). From this figure, we found that (1) TiO_2–ZrO_2 catalysts with 50–75 mole% of TiO_2 had the highest $ZrTiO_4$ content; (2) considerable amount of ZrO_2 occurred along with $ZrTiO_4$ when the content of TiO_2 was less than 25 mole%. As mentioned previously, the formation of crystalline $ZrTiO_4$ and the amounts of acid and base are the major factors affecting the activity of this reaction, we expect that catalytic activity of TiO_2–ZrO_2 with 25 mole% of TiO_2 should be lower than that of 50–75 mole%. The results shown in Fig. 9 substantiate this expectation.

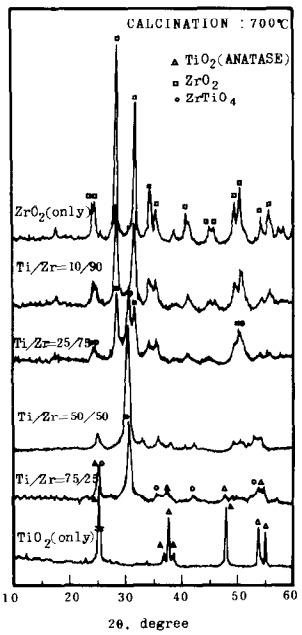

FIG. 11. X-Ray diffraction pattern of TiO_2–ZrO_2 at various compositions.

Figure 12 shows the amount of ethylbenzene adsorption as a function of the calcination temperature for TiO_2–ZrO_2 (1/1). The amount of ethylbenzene adsorption decreased with increasing calcination temperature. These results correlated well with the change in the amounts of acid and base shown in Fig. 1. From Figs. 12 and 1, we knew that the catalyst calcined at 650°C did not show the maximum adsorption, but it did show the maximum activity. These results also indicate that the maximum activity of catalyst obtained by calcination at 650°C is due to the properly oriented acidic and basic sites, i.e., the formation of crystalline $ZrTiO_4$.

Effect of Pretreatment with H_2, O_2, and Steam

According to Tanabe's hypothesis (*19*), structures **I** and **II** could be the structures of mixed metal oxide, TiO_2–ZrO_2, with TiO_2 or ZrO_2 as the major component, respectively. The solid S, which contains hy-

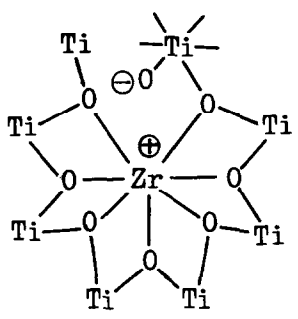

(I)

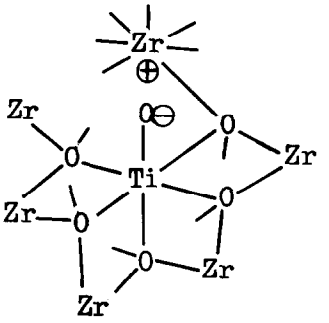

(II)

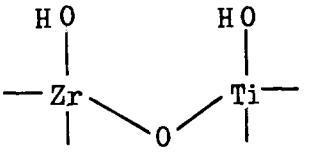

(III)

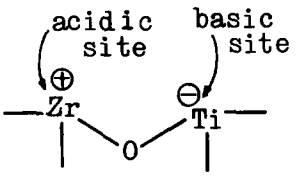

(IV)

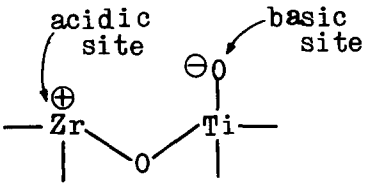

(V)

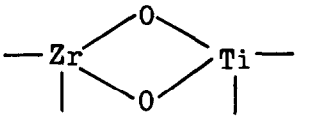

(VI)

droxide groups, is expected to have the amorphous form of structure **III**. This structure changes to structures **V, IV,** and **VI** as calcination temperature increases. As pointed out previously, the formation of crystalline $ZrTiO_4$ occurred at calcination temperatures above 650°C, and the rutile structure was formed gradually, when the calcination temperature was above 850°C. The amounts of acid and base decreased with increasing calcination temperature. Based on these considerations, the possible surface structures of catalyst H, E, A, I, and J, which were obtained from solid S after 550, 600, 650, 700, and 1000°C calcination, are proposed and shown in Scheme 2.

The activities and yield of styrene for the reactions over these catalysts are shown in Fig. 2. Catalyst A which was obtained after 650°C calcination gives the maximum activity and yield of styrene. It may be due to the formation of crystalline $ZrTiO_4$ and the amounts of acid and base as mentioned above. Some of crystal structure **VI** was formed along with the formation of crystal **IV** and **V** when the solid S was calcined above 700°C. The phenomena of phase separation, i.e., the formation of rutile structure, was found in catalyst J which was obtained by calcination at 1000°C. Therefore, the surface area, total amounts of acid and base, and the activity of ethylbenzene dehydrogenation of the catalysts decrease as the calcination temperature increases as shown in Figs. 1 and 2.

In an attempt to find out the possible structures of the active sites and the role of

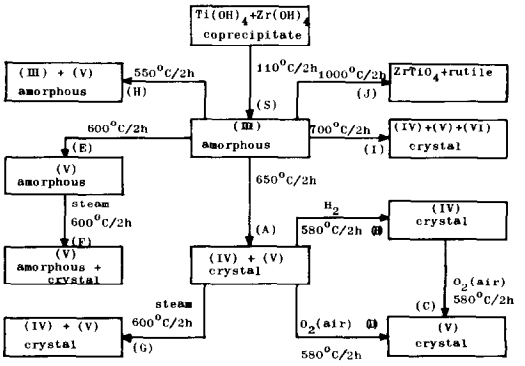

SCHEME 2

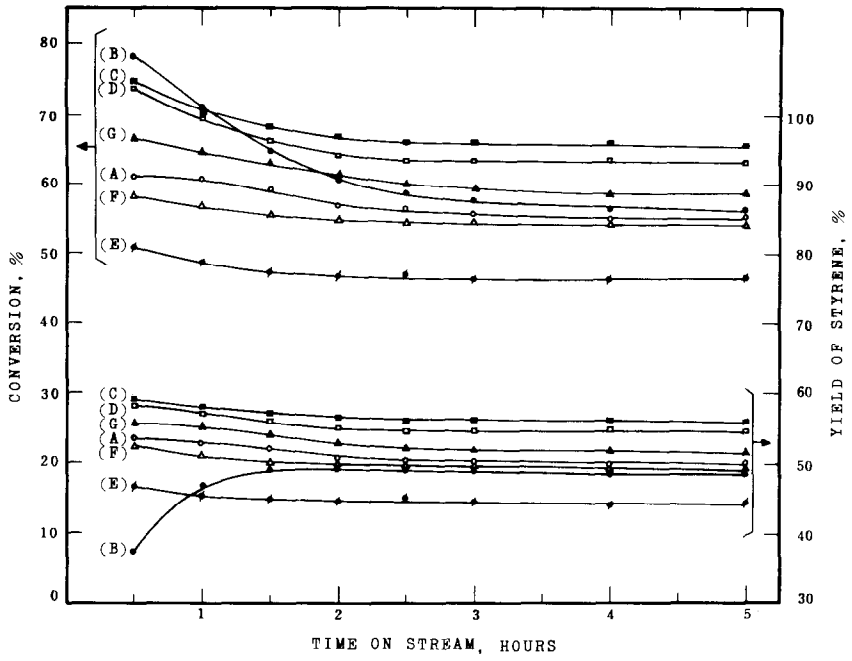

FIG. 13. Effect of pretreatment on the total conversion and the yield of styrene. (A), (B), (C), (D), (E), (F), and (G) are obtained as shown in Scheme 1.

crystalline $ZrTiO_4$ for ethylbenzene dehydrogenation over TiO_2–ZrO_2 catalysts, the catalysts were pretreated with H_2, O_2 (air), or steam as described in Scheme 1. The catalytic activities were measured under the same conditions as described above. All of the catalysts were purged with N_2 at 580°C before activity test. The results are shown in Fig. 13.

Catalyst B was obtained by the pretreatment of catalyst A with H_2 at 580°C for 2 hr, and showed higher initial activity but lower selectivity than catalyst A. They reached almost the same activity and selectivity after 5 on-stream hr. When catalyst A was pretreated with H_2 at 580°C for 2 hr and then reoxidized with air at the same temperature, catalyst C was obtained which showed higher activity than catalysts A and B. Catalyst D, which was obtained by the pretreatment of catalyst A with air directly showed higher activity than catalyst A and slightly lower activity than catalyst C. The results are shown in Fig. 13.

Based on these results, we proposed that catalyst B might be in crystal form of structure **IV**, and the part with structure **V** in catalyst A was reduced to structure **IV** as expressed in

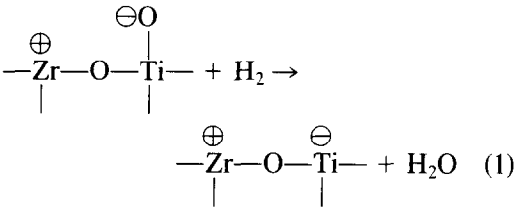

The oxidation states of titanium at the basic sites in structures **IV** and **V** are 2+ and 4+, respectively. The larger amount of benzene formation at the initial time for catalyst B may be due to the removal of oxygen by H_2 from

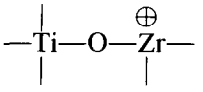

The removal of oxygen causes the reduction of titanium and the increasing of posi-

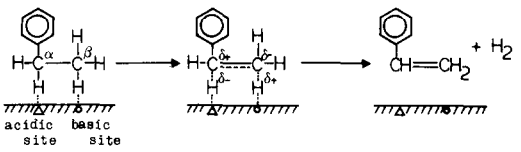

FIG. 14. Acid–base bifunctional mechanism proposed for the nonoxidative dehydrogenation of ethylbenzene.

tive charge on zirconium as expressed in

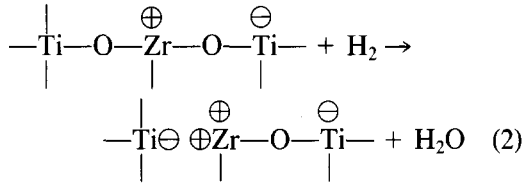

(2)

and therefore, the increasing of acidity which was considered to be active sites for cracking.

Catalysts C and D proposed to be in crystal form of structure **V**. They showed higher activity and selectivity than catalysts A and B after 5 on-stream hr. The part with structure **IV** in catalyst A was oxidized or reoxidized to structure **V** when treated with air. It is concluded that structure **V** is more reactive than structure **IV** for ethylbenzene dehydrogenation. The possible explanations are that the basicity of

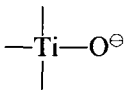

is higher than that of

and that structure **V** has the properly oriented sites for the concerted two-center mechanism as shown in Fig. 14. Therefore, structures IV and V are proposed to be the active sites for ethylbenzene dehydrogenation over TiO_2–ZrO_2 catalysts.

Catalysts F and G were obtained from catalysts E and A, respectively, by calcination with steam at 600°C for 2 hr. The activity of catalyst F is similar to that of catalyst A, and both of them are superior to that of catalyst E. The activity of catalyst G is slightly higher than that of catalyst A, but smaller than those of catalysts C and D. XRD analysis showed that catalyst E was amorphous while catalyst F, which was obtained by treating with steam, was partially crystallized. Accordingly, we propose that catalyst F consists of structure **V** in both amorphous and crystal forms. The activity of catalyst G is higher than that of catalyst A. This difference may be due to that the content of structure **V** on catalyst G is higher than that on catalyst A. This reactivity order indicates that the pretreatment with steam at 600°C is beneficial for the formation of crystalline $ZrTiO_4$, and that structure **V** is more reactive than structure **IV**.

From the above discussion, we conclude that nonoxidative dehydrogenation of ethylbenzene over TiO_2–ZrO_2 catalysts undergoes an acid–base bifunctional mechanism. The formation of crystalline $ZrTiO_4$ by raising the calcination temperature (>650°C) or by the pretreatment with steam at 600°C will be beneficial for the catalytic activity. Structures **IV** and **V** are proposed to be the acid–base bifunctional active sites, and structure **V** is more reactive than structure **IV**. The properly oriented acidic and basic sites of crystalline $ZrTiO_4$ could facilitate the concerted two-centered attack of α-H and β-H of ethylbenzene, respectively. Thus we propose that the content of crystalline $ZrTiO_4$ as well as the amounts of acid and base are the major factors affecting the catalytic activity for nonoxidative dehydrogenation of ethylbenzene.

ACKNOWLEDGMENTS

The authors express their gratitude for the support of this work by the National Science Council of the Republic of China and the Refining and Manufacturing Research Center of Chinese Petroleum Corporation.

REFERENCES

1. Arata, K., Akutagawa, S., and Tanabe, K., *Bull. Chem. Soc. Jpn.* **49**(2), 390 (1976).

2. Araka, K., and Tanabe, K., *Bull. Chem. Soc. Jpn.* **53,** 299 (1980).
3. Wang, I., Chang, W. F., Shiau, R. J., Wu, J. C., and Chung, C. C., *J. Catal.* **83,** 428 (1983).
4. Tagawa, T., Hattori, T., and Murakami, Y., *J. Catal.* **75,** 56 (1982).
5. Tagawa, T., Hattori, T., and Murakami, Y., *J. Catal.* **75,** 66 (1982).
6. Simonik, J., and Pines, H., *J. Catal.* **24,** 211 (1972).
7. Pines, H., and Kobylinski, T. P., *J. Catal.* **17,** 375 (1970).
8. Licht, E., Schächter, Y., and Pines, H., *J. Catal.* **61,** 109 (1980).
9. Pines, H., *J. Catal.* **78,** 1 (1982).
10. Lynch, R. W., and Morosin, B., *J. Amer. Ceram. Soc.* **55**(8), 409 (1972).
11. Newnham, R. E., *J. Amer. Ceram. Soc.* **50**(4), 216 (1967).
12. Noguchi, T., and Mizuno, M., *Sol. Energy* **11**(1), 56 (1967).
13. Mizuno, M., and Noguchi, T., *Nagoya Kogyo Gijutsu Shikensho Hokoku* **13,** 124 (1964).
14. Mizuno, M., Noguchi, T., and Naka, S., *Nagoya Kogyo Gijutsu Shikensho Hokoku* **12,** 385 (1963).
15. Belyaev, I. N., and Ivleva, T. I., *Izv. Vyssh. Uchebn. Zaved., Khim Khim. Tekhnol.* **22**(3), 382 (1979).
16. Walvekar, S. P., and Halgeri, A. B., *Indian J. Chem.* **11**(7), 662 (1973).
17. Limar, T. F., Kagan, Y. A., and Isaeva, V. F., *Izv. Akad. Nauk SSSR, Neorg. Mater.* **14**(1), 112 (1978).
18. Powder diffraction file, Inorganic, No. 21-1276, 21-1272, and 7-290.
19. Tanabe, K., Sumiyoshi, T., and Shibata, K., *Bull. Chem. Soc. Jpn.* **47**(5), 1064 (1974).